Asian Journal of Chemistry; Vol. 30, No. 6 (2018), 1221-1227

ASIAN JOURNAL OF CHEMISTRY

https://doi.org/10.14233/ajchem.2018.21157

Structural Elucidation of Borate Glasses by Spectroscopic and SEM Studies

S. THIRUMARAN* and A. PRIYADHARSINI

Department of Physics, Annamalai University, Annamalai Nagar-608 002, India

*Corresponding author: E-mail: thirumaran64@gmail.com

Received: 6 December 2017; *Accepted*: 16 January 2018; *Published online*: 30 April 2018; AJC-18869

Glass samples of composition (B_2O_3-WO_3-Bi_2O_3) BTB glass systems and (B_2O_3-SiO_2-Bi_2O_3) BSB glass systems with ranging from 2 mol % are prepared by melt quenching technique. The structural analysis of glasses is analyzed by Fourier-transform infrared, UV-visible and scanning electron microscopy studies. The FTIR spectrum identifies the broad absorption bands indicated the wide distribution of borate structural units. The UV-visible study observes the increasing band gap energies of glass specimen suggesting their nature of rigidity. The surface morphological aspects of the prepared glass samples are examined by scanning electron microscopy study.

Keywords: Borate glass, Spectroscopic studies.

INTRODUCTION

Fourier transform infrared (FTIR) technique is one of the most sought spectroscopic tool to probe the structural units present in the glass matrix. It is one of the most useful experimental techniques providing the information about the arrangement of building structural groups with respect to each other and types of bonds present in the glass [1]. The IR spectra of glasses are used to get more information about the presence of different structural groups. UV-visible spectrum occurs due to the electronic transition of the molecules for determining the absorption edge and band gap energies of the investigated materials.

When a semiconductor absorbs photon of energy larger than the gap of semiconductor, an electron in transferred from the valence band to the conduction band, where there occurs an abrupt increase in the absorbency of the materials to the wavelength corresponding to the band gap energy whether the electronic transition is direct or indirect. UV-visible DRS help to obtain the optical band gap energies, the experimental data, assuming direct and indirect band transitions [2]. The aim of the present work is to investigate the physical, structural characterization of ternary glass systems with WO_3, SiO_2 and Bi_2O_3 doped with borate are probed by using Fourier transform infrared spectroscopy and UV-visible spectroscopy measurements. The surface morphological aspects of glass specimen was also evaluated by scanning electron microscopy study.

EXPERIMENTAL

The chemicals used in the present study for the preparation of glass specimen were obtained from the standard and companies. The glass composition was prepared in mole percentage (mol %) with increasing content of borate with decreasing content of Bi_2O_3 in (B_2O_3-WO_3-Bi_2O_3) BTB glass systems and the same with decreasing content of Bi_2O_3 in (B_2O_3-SiO_2-Bi_2O_3) BSB glass systems where the mole percentage increased in steps of 2 mol % have been prepared by using the conventional melt quenching technique. The proper compositions were mixed together by grinding the mixture repeatedly to obtain a fine powder. The mixture is melted in silica crucible and melting was carried out under temperature controlled muffle furnace with occasional stirring. The temperature controlled furnace was gradually raised to a higher temperature at the rate of 373K per hour and a glassy structure was noticed at 1303K for BTB glass systems and 1353K for BSB glass systems, respectively.

Eventually the molten glass melt was immediately poured on a heavy copper molding block having dimensions 12 mm diameter and 4 mm thickness kept at room temperature. Then the glass samples were annealed at 673K for 2 h to avoid the mechanical strains developed during the quenching process. Later glass specimen were allowed to cool gradually at room temperature. The prepared glass samples were polished and their surface is made perfectly plane and smoothened.

The FTIR transmission spectra of the glass samples were recorded at room temperature using KBr pellet technique with a spectrum RX-1 FTIR spectrometer (Perkin Elmer, USA) in the spectral range 4000-400 cm^{-1}. The prepared glass samples were thoroughly mixed with dry KBr with the ratio 1:100 mg glass powder to KBr, respectively. The weighed mixtures were then subjected to a pressure of 5 tons/cm^2 to produce clear homo-

geneous discs. The IR measurements were immediately carried out after preparing the discs. For UV-visible studies, the glass samples were finely ground in an agate pestle and mortar. Diffuse reflectance spectra of the samples under investigation were taken using UV1600 series Shimadzu spectrophotometer at room temperature. The relative diffuse reflectance was measured with $BaSO_4$ powder taken as reference. The morphology of the samples was examined using scanning electron microscope with an acceleration voltage of 20 kv and working distance of 20-26 mm at high vacuum (HV) mode. The materials for investigation is hot air oven dried for about 1 h at 110 ºC , then coated with the help of gold coater using JEOL auto fine coater model JES-1600, coating time is 120 s,10 mA and deposited with a thin layer of gold on the sample and later taken for examination.

RESULTS AND DISCUSSION

Fourier-transform infrared studies: The FTIR transmittance spectra of BTB (B_2O_3-WO_3-Bi_2O_3), and BSB (B_2O_3-SiO_2-Bi_2O_3) glass system were recorded over the range of 4000-400 cm^{-1} (Fig. 1). The FTIR spectroscopy of borate containing compounds has vibrational modes mainly active in three infrared spectral regions (i) 1600-1200 cm^{-1} group of bands which are due to the asymmetric stretching relaxation of B-O bond of trigonal BO_3 units (ii) bands in the range 1200-800 cm^{-1} due to B-O bond stretching of tetrahedral BO_4 units and (iii) peaks around 700 cm^{-1} due to bending of B-O-B linkages in the borate networks [3]. The bands in the range 3600-3200 cm^{-1} are attributed to the hydroxyl or water groups originating from molecular water [4]. The key band assignments of all peaks in BTB and BSB glass systems are reported in Tables 1 and 2, respectively. The broad bands are due to the overlapping of individual bands having its characteristic to some type of vibration of a specific structure. The group and its relative area which is proportional to the concentration of this structural group. The boron atom in borate glasses is usually coordinate with either 3 or 4 oxygen atoms forming BO_3 (or) BO_4 units. These two fundamental units can be combined to form either super structural units or different B_xO_y groups like boroxol rings, pentaborate, tetraborate and diborate groups.

In BTB glass system, the increase of B_2O_3 contents causes a increasing of the absorbance in the range 1400-700 cm^{-1} corresponding to more polymerized structural units. This feature

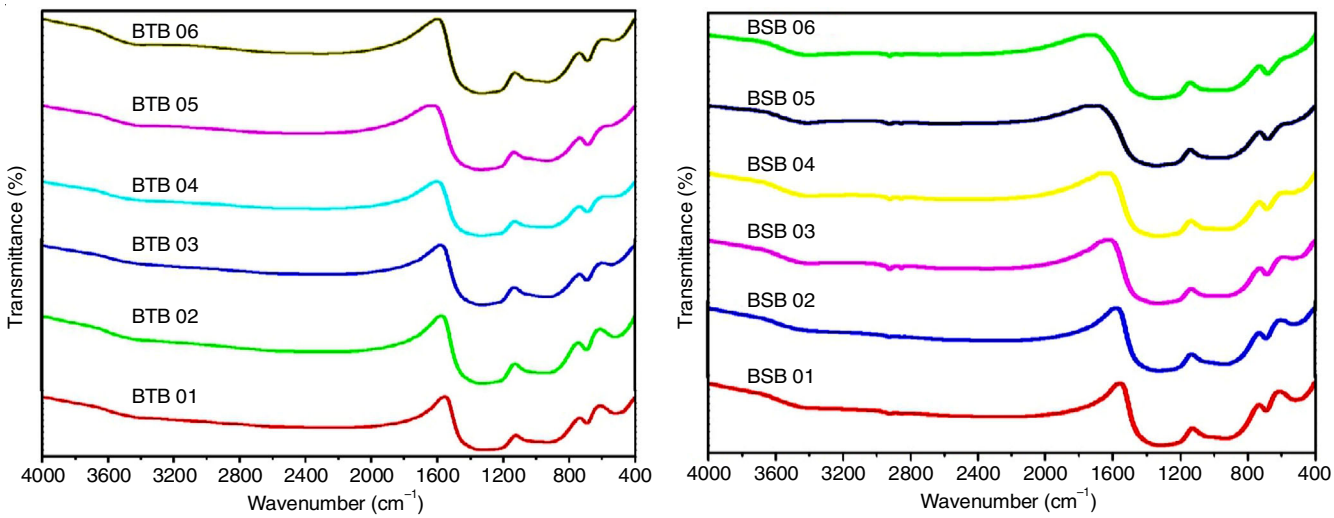

Fig. 1. FTIR specrum for (a) BTB glass system, (b) BSB glass system

TABLE-1
BAND ASSIGNMENTS OF BTB GLASS SYSTEM
System-I: B_2O_3-WO_3-Bi_2O_3 (BTB-Glass system)

Wavenumber (cm^{-1})	Band assignment
557-511	Bi-O and Bi-O-Bi stretching vibrations of [BiO_6] octahedral structural units.
695-689	The band bending vibration of B-O-B linkages of the boron –oxygen network between two trigonal boron atoms in BO_3 triangles.
943-931	The stretching vibrations of B-O linkages in BO_4 tetrahedra overlapping with the stretching vibrations of WO_6 units.
1336-1324	B-O stretching vibrations of trigonal units.
3401-2234	Hydroxyl or water group originating from molecular water.

TABLE-2
BAND ASSIGNMENTS OF BSB GLASS SYSTEM
System-II: B_2O_3-SiO_2-Bi_2O_3 (BSB-Glass system)

Wavenumber (cm^{-1})	Band assignment
542-519	Bi-O and Bi-O-Bi stretching vibrations of in [BiO_6] octahedral structural units.
693-685	The bond oxygen network between two trigonal boron atoms in BO_3 triangles.
943-928	The Si-O stretching vibration in SiO_4 tetrahedral units with non- bridging oxygen atoms.
1343-1319	B-O stretching of tetrahedral BO_4 units
3402-2853	The absorption bands due to vibrations of water, hydroxyl (OH).

clearly indicates an increasing of the number non-bridge oxygen's. In particular, the atmospheric moisture is easily absorbed by the pellet causing the appearance of IR band belonging to H_2O molecules. The IR spectra of the existing structural borate groups and their arrangement are absorbed to be slightly affected by the change of glass composition and their intensities also show minor variations.

The IR peak in the region 557-511 cm^{-1} may be attributed to Bi-O and Bi-O-Bi stretching vibrations of [BiO_6] octahedral structural units [5]. As B_2O_3 is a well known network former with BO_3 structural units and hence its presence of BO_4 units is evident in this glass from FTIR spectral studies. The band bending vibration of B-O-B linkages of boron-oxygen network between two trigonal boron atoms in BO_3 triangles appear in the spectra at 695-689 cm^{-1} for various concentrations [6]. The present IR spectra showed non-existence of band at 806 cm^{-1}, which reveals the absence of boroxol rings in glasses and hence it consists of only BO_3 and BO_4 groups [7]. WO_3 is a metal oxide, which do not form glasses by themselves but do so readily in combination with other glass formers like B_2O_3. Tungsten ions are well known for their unusual influence on optical and electrochemical properties of glasses for the simple reason than the oxides of tungsten participate in glass network with different structural units like WO_4 and WO_6 [8] .

The role of WO_3 that induces the well defined band at 943-931cm^{-1} from BTB-1 to BTB-6 glass system which is assigned to the stretching vibrations of B-O linkages in BO_4 tetrahedra overlapping with the stretching vibrations of WO_6 units [9]. There is no significant change in position of these bands. The change in intensity and wave number due to the presence of W-O-W vibration in the glass network and also due to WO_4 units of tungsten. The peak 943 cm^{-1} is assigned to the stretching vibrations W-O band associated with WO_4 and WO_6 units. This indicates that tungsten enter the glass structure. The peaks at the range 1336-1324 cm^{-1} from BTB-1 to BTB-6 glass due to B-O stretching vibrations of trigonal units [10]. The peak at 3401-2234 cm^{-1} attributed to hydroxyl or water group originating from molecular water [11]. The lack of sharp peak is indicative of the general disorder in the borate network mainly due to a wide distribution of Bi_2O_3 or WO_3 units occurring in this glass. Bi_2O_3 is a weak glass former and it participates in the glass network with triangular BiO_3 pyramidal units. All the above vibration assignments are in good agreement with literature survey since WO_3 in a conditional glass former with the substitution of WO_3 vibrate glass network. The infrared spectra of our second ternary (B_2O_3-WO_3-Bi_2O_3) BSB glass system showed that addition of Bi_2O_3 causes broad absorption band axis in the region 1100-850 cm^{-1}. Bands in this region are not observed in the infrared spectra of pure B_2O_3 glasses. Earlier studies reporting the partly role of Bi_2O_3 as network former in the glass system. Moreover, Bi^{3+} posses lone pair electron in the outer most orbit. Thus, the structural role played by Bi_2O_3 in silicate/borate glasses is complicated and imperfectly understood. B_2O_3 is one of the most common glass former and is present in almost all commercially important glasses because of its high strength the ability of boron exists three and four oxygen coordination environments and the high strength of covalent B-O bond enables to form stable glasses.

From the observed bands of the IR spectra, it is clear that the expected structural units that build the glass network of the investigated samples are [BiO_3] pyramidal, [BiO_6] octahedral and [SiO_4] tetrahedral units. On the other hand, Bi_2O_3 is not a classical glass former but in the presence of conventional glass formers like SiO_2, PbO and B_2O_3, a glass network of BiO_3 and BiO_6 units may be built [12]. This is because the [BiOn] polyhedra are highly distorted due to the presence of lone pair electrons. Also Bi_2O_3 possess asymmetrical structural units in the crystal state and it is possible to form bond with different lengths in distorted polyhedral. Further, Batal [13] have studied the IR spectra, thermal properties and density values of Bi_2O_3, SiO_2 glasses and observed the sharing of Bi^{3+} in network glass structure as octahedral BiO_6 groups and the possibility of presence of BiO_3 units. The peak at 519 cm^{-1} BSB-1 glass shifted to a higher wave number side as the B_2O_3 content increases and reaches at 542 cm^{-1}, and this peak is attributed to the various modes of Bi-O and Bi-O-Bi stretching vibrations of [BiO_6] octahedral structural units [14]. The bond oxygen network between two trigonal boron atoms in BO_3 triangles appears in FTIR spectra at 696-685 cm^{-1} for BSB-1 to BSB-6 glasses [15]. The peaks observed in the range 943-928 cm^{-1} are attributed to the Si-O stretching vibration in SiO_4 tetrahedral units with non-bridging oxygen atoms [16]. B-O stretching of tetrahedral BO_4 units appears in the BSB-1 glass at 1319 cm^{-1} and in the BSB-6 glass at 1343 cm^{-1} [17]. The bands located at 4000-2000 cm^{-1} comprises the absorption bands due to vibrations of water, hydroxyl (OH) [18]. The peaks at 519, 685, 928 and 1319 cm^{-1} in BSB-1 glass shifted to a higher wave number side and the intensity of the peaks slightly decrease as the amount of Bi_2O_3 in glass decrease. Hence, in the present system Bi_2O_3 and WO_3 play the role of both network modifier and former. Consolidating the overall our two glass systems, the FTIR study eventually confirms the presence of various contents of borate network.

UV-visible DRS studies: Diffuse reflectance spectroscopy (DRS) is a simple, but powerful spectroscopic tool to estimate the band gap energy (E_g) of powder samples unambiguously. As the technique does not require the sample to be dispersed in a liquid medium, the material is not contaminated [19]. Band gap is generally obtained from optical absorption edge energy, which is defined as the minimum photon energy required to excite an electron from the highest occupied molecular orbital (HOMO, at the top of the valence band in semiconductor domains) to the lowest unoccupied molecular orbital (LUMO, at the bottom of the conduction band) [20]. Electronic transitions are of two types *viz*., direct and indirect. Direct transitions require only that photons excite electrons, whereas indirect transitions require vibrations and energy from the crystal lattice (phonons). Kubelka-Munk (KM) theory provides the theoretical descriptions of diffuse reflectance spectroscopy [21-23]. When the powdered sample is radiated with light, a portion is regularly reflected at a powder surface and the remaining enters the powder and diffuses. As light of particular wavelength is absorbed by the sample, the measurement of the diffuse reflected light at different wavelengths yields a spectrum called diffuse reflectance spectrum. The calculated values of absorption edge or cut-off wavelengths and band gap energies for BTB and BSB glass systems are given in Table-3.

TABLE-3
CUTOFF WAVELENGTH AND BAND GAP ENERGY FOR BTB AND BSB GLASS SYSTEMS

Sample	System-I: B_2O_3-WO_3-Bi_2O_3				Sample	System-II: B_2O_3-SiO_2-Bi_2O_3			
	Cutoff wavelength	Theoretical values of band gap (eV)	Band gape E_g (eV)			Cutoff wavelength	Theoretical values of band gap (eV)	Band gape E_g (eV)	
			Direct	Indirect				Direct	Indirect
BTB-1	330	3.75	3.35	2.90	BSB-1	318	3.89	3.49	3.11
BTB-2	327	3.79	3.40	3.04	BSB-2	316	3.92	3.52	3.12
BTB-3	325	3.81	3.45	3.06	BSB-3	315	3.93	3.56	3.14
BTB-4	322	3.85	3.46	3.08	BSB-4	314	3.94	3.60	3.16
BTB-5	321	3.86	3.49	3.10	BSB-5	312	3.97	3.65	3.25
BTB-6	320	3.87	3.50	3.18	BSB-6	301	4.11	3.68	3.27

For the prepared two glass systems (BTB and BSB glass systems), the cut-off wavelength was determined by plotting a graph between the reflectance (R) in percentage *versus* wavelength (λ) in nm as shown in Fig. 2. The reflectance spectrum of these two glass spectrum are taken in the visible region of ranging from 200 nm upto 700 nm.

From Fig. 2 and Table-3, one could see that the cut-off wavelengths decrease for both glass systems and shift towards the blue shift of the wavelength *i.e*. towards lower wavelength side. The optical band gap in the glass specimen was determined by using the relationship Kubelka-Munk function [24] (eqn. 1).

$$F(R) = \frac{(1-R)^2}{2R} \quad (1)$$

where R is the absolute value of reflectance and F(R) is equivalent to the absorption coefficient. Using the Kubelka-

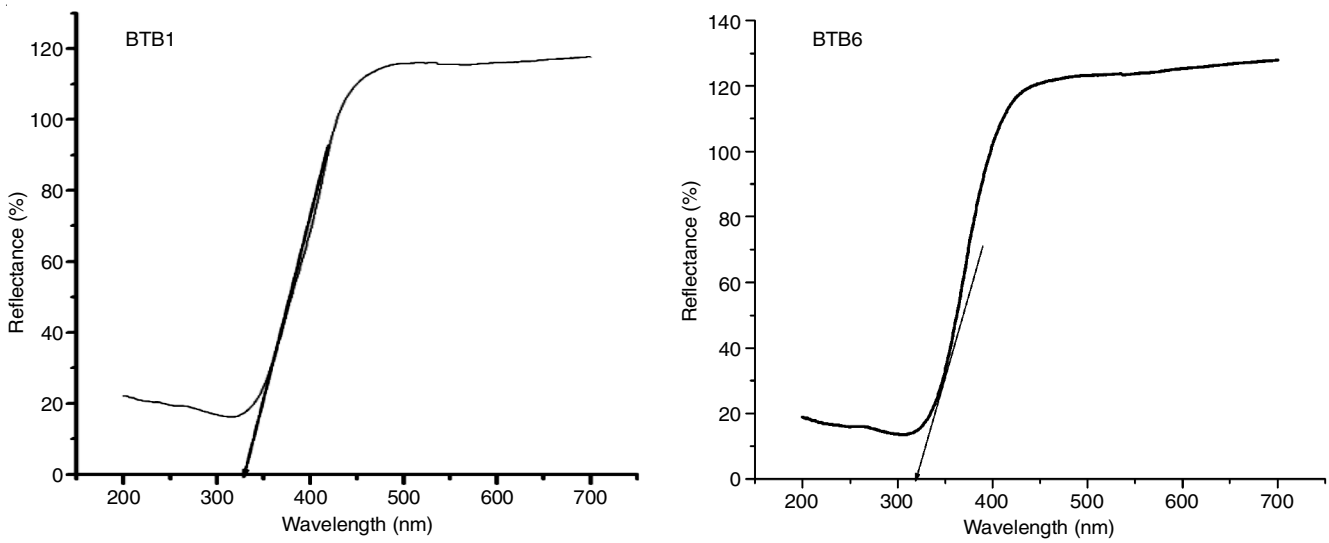

Fig. 2a. Diffuse reflectance spectra of BTB-1 and BTB-6 glass samples in BTB glass systems

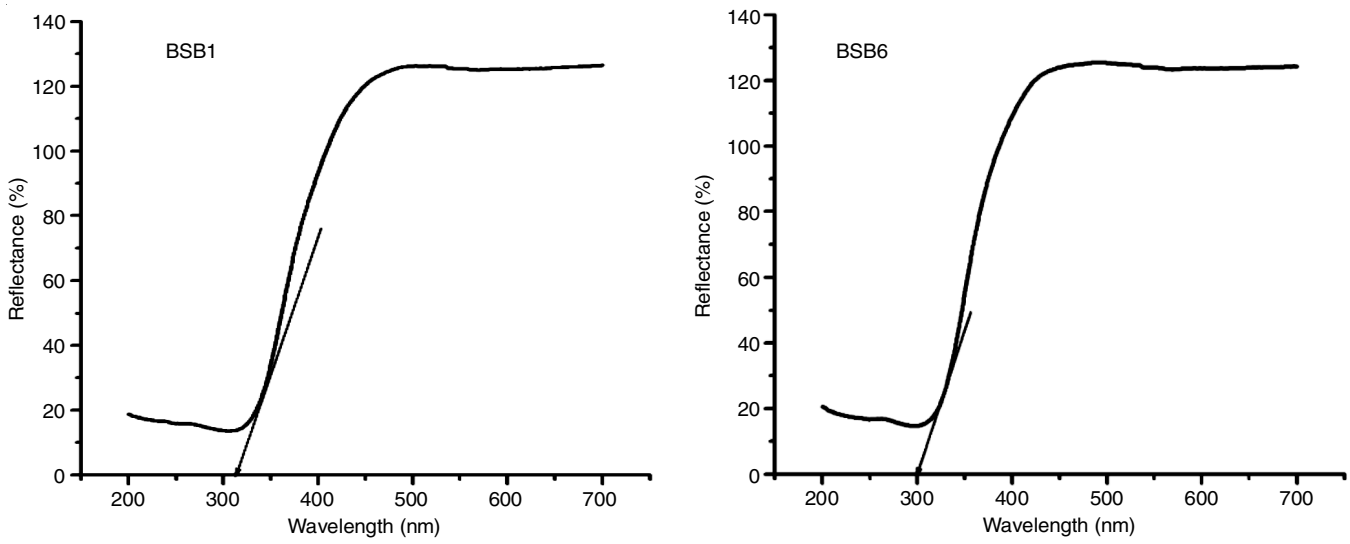

Fig. 2b. Diffuse reflectance spectra of BSB-1 and BSB-6 glass samples in BSB glass systems

Munk function, the $[h\nu.F(R)]^2$ was plotted against hν. The direct band gap energy was calculated by the curve that plots the value of $[h\nu - (F(R).h\nu)^2]$ on the horizontal axis hν and vertical axis $(F(R).h\nu)^2$ is drawn. A line drawn tangent to the point of inflection on the curve and the hν value at the point of intersection of tangent line and the horizontal axis is the band gap E_g value. The indirect band gap energy was calculated by plotting $[F(R).h\nu]^{0.5}$ *versus* energy (hν) [25,26] is presented for BTB and BSB glass systems in Fig. 3.

From the present UV-visible DRS measurements, it is seen that the band gap values increases around 3.35 to 3.50 eV for BTB glasses for direct method and 2.90 eV to 3.18 eV for indirect and similarly for BSB glasses found around 3.49 to 3.68 eV for direct method and 3.11 to 3.27 eV indirect method. Their anomalous behaviour of the variation in optical band gap can be explained on the basis of decrease or increase in non-bridging oxygen (NBO) content in the glass network [27]. From the evaluated both direct and indirect transitions, it is clear that the increase of band gap energies observed for both glass systems. Interestingly in the direct transition the increasing of band gap energy is seen more distinctly comparing to indirect transition. Optical absorption is a useful method for investigating optically induced transition and to get information about the bond structure and energy gap of non-crystalline materials.

The present investigation through UV-visible study finds that (i) increasing of band gap energy for both glass systems and (ii) decreasing of cut-off wavelength. Increasing band gap suggests a poor rigidity of the glass network after irradiation. This result further supported by the observed blue-shift of the cut-off wavelength (towards lower wavelength side) [28]. In addition, the increasing band gap can be attributed to the decreasing of non-bridging oxygen atoms after breaking the bonds between boron and oxygen atom. For the amorphous materials, the values of the band gap energy are above 3 eV independent of the transition types [29]. Our measured direct and indirect transition values exhibit more than 3 eV, confirming the amorphous nature of the glass specimen and this increasing of band gap energy is resulting in decreasing of non-bridging oxygen atoms in the glassy matrix [30,31]. The increasing band gap can be attributed that there is an increasing number of energetic electrons in the glass network with increasing of borate content. This electronic ionization will increase the electronic transition between localized states, so that the band gap increases. It may also further be interpreted as, for the band gap increase it may

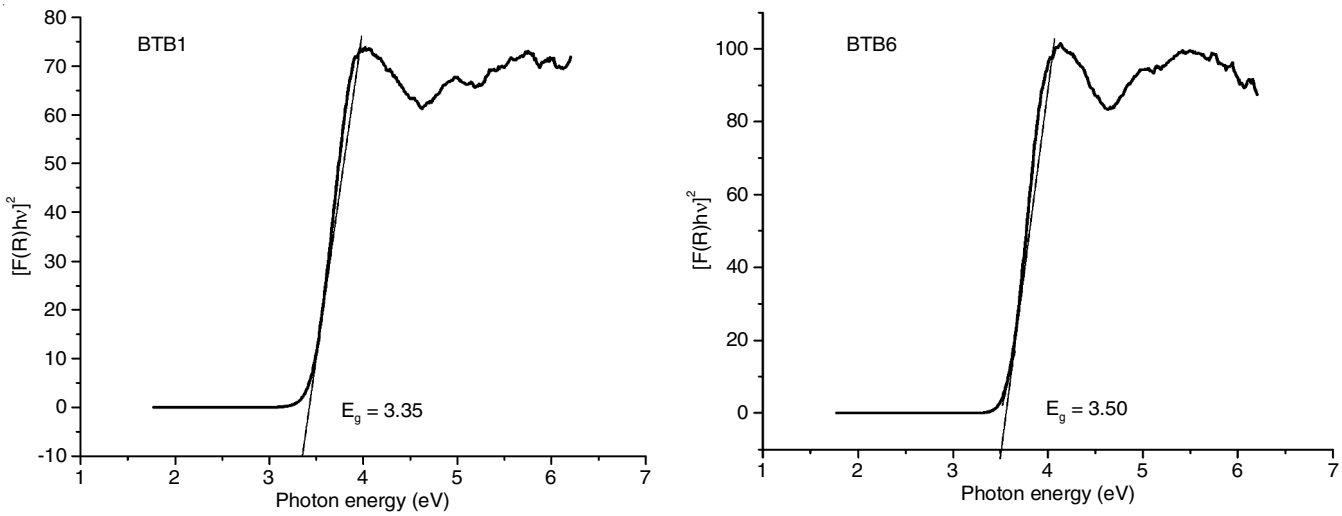

Fig. 3a. Photon energy (eV) *versus* $[F(R)h\nu]^2$ graph of BTB-1 and BTB-6 glass system (Direct)

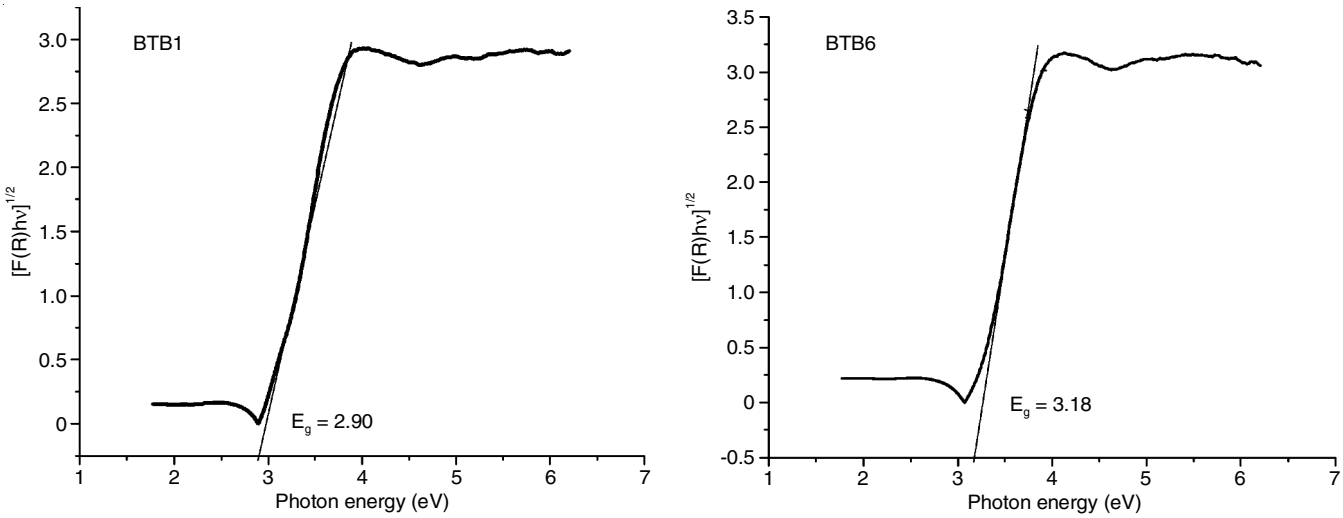

Fig. 3b. Photon energy (eV) *versus* $[F(R)h\nu]^{1/2}$ graph of BTB1 and BTB6 glass system (Indirect)

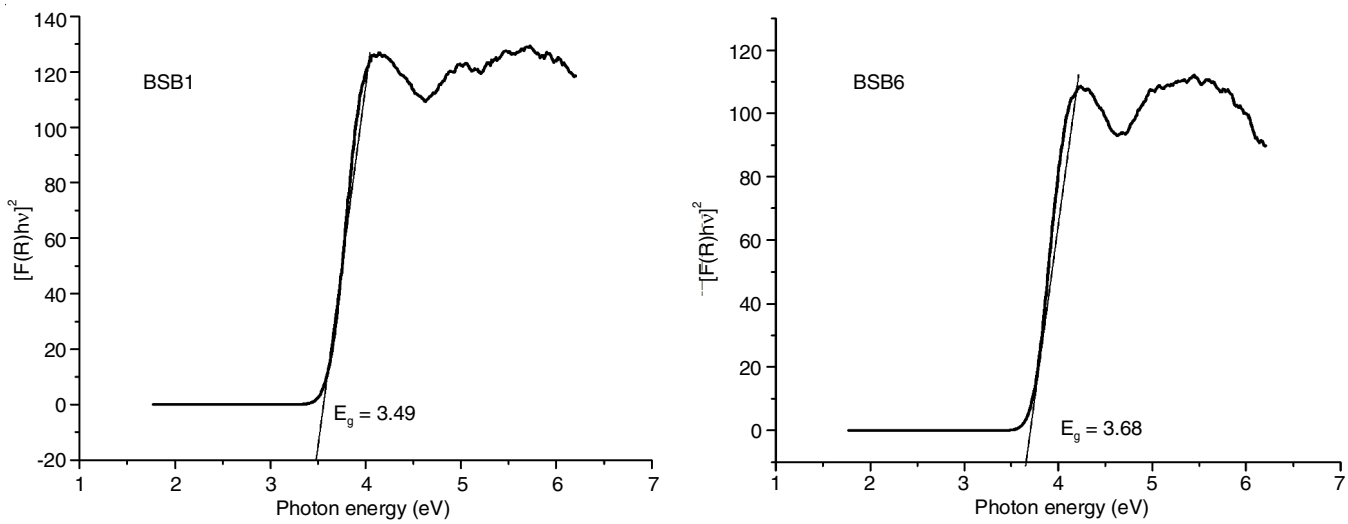

Fig. 3c. Photon energy (eV) *versus* $[F(R)h\nu]^2$ graph of BSB-1 and BSB-6 glass system (Direct)

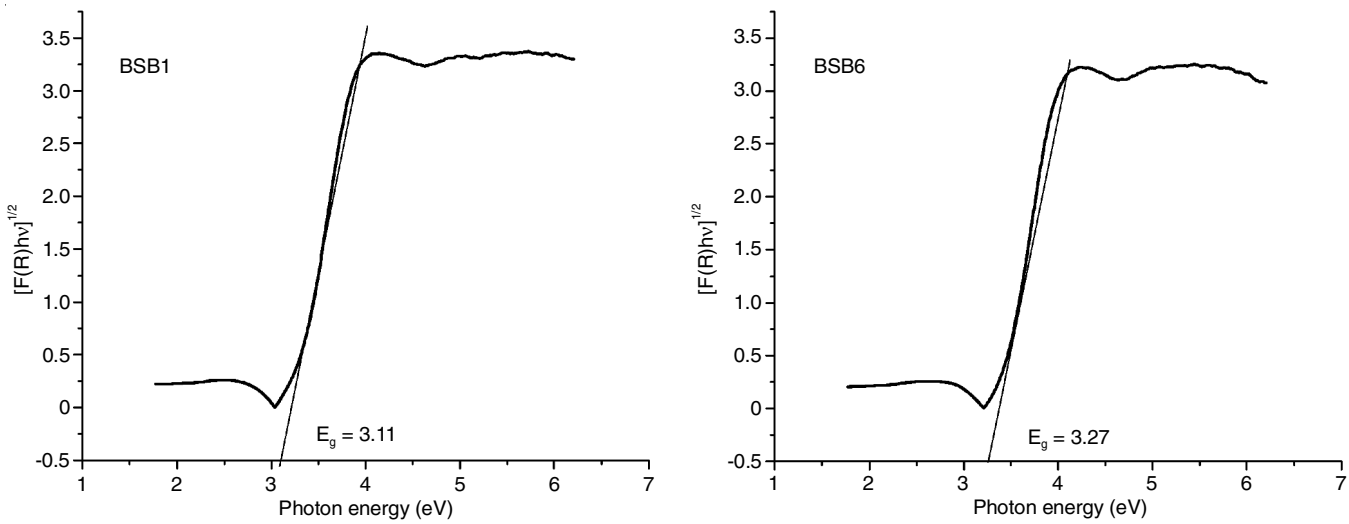

Fig. 3d. Photon energy (eV) *versus* $[F(R)h\nu]^{1/2}$ graph of BSB-1 and BSB-6 glass system (Indirect)

due to high doped concentrations which causes the broadening of the impurity band and the formation of bond tails on the edges of conduction and valence bands [32].

Scanning electron microscopic (SEM) studies: The magnified images of BTB and BSB glasses are shown in Fig. 4. It is observed that the sample exhibits surfaces without microstructure and different sized grain particles are distributed. The particle (grain) sizes vary in each micrograph and the glass surface due to the deposition of amorphous apatite, confirming its amorphous nature. From Table-3, it is seen that band gap energy values are comparatively high in SiO_2 doped glass system than WO_3 glass system indicating that as explained in UV studies. This attributes poor rigidity in glassy matrix is noticed in BTB glass system. The SEM analysis found densely packed grains free from holes, suggested that during glass formation, the presence of clusters composed of fibers is formed. The glass may consist aggregates, agglomerates and clusters, which clearly explain the surface of morphology of glass samples. The prepared glass samples contain well defined randomly distributed ingrained in a glassy network. The residual glass phase is acting as interconnecting zones making the glass samples free of voids and cracks.

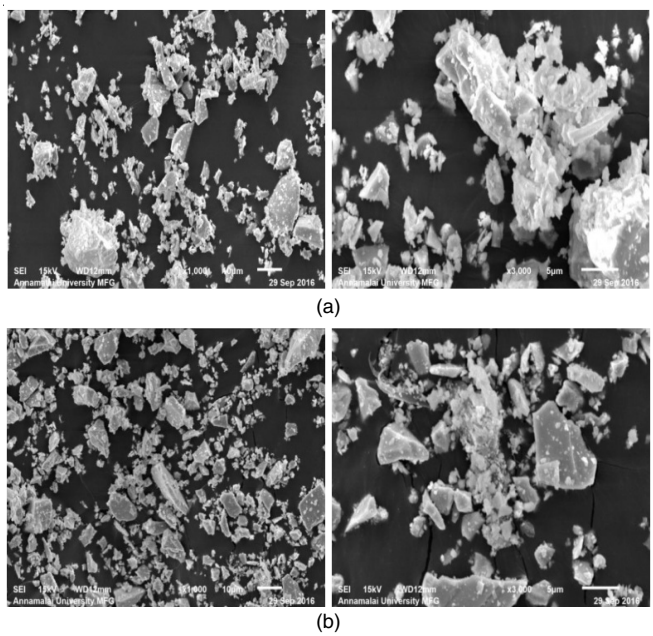

Fig. 4. SEM analysis of (a) BTB glass sample and (b) BSB glass sample

Conclusion

In this work, several glass samples of composition (B_2O_3-WO_3-Bi_2O_3) BTB glass systems and (B_2O_3-SiO_2-Bi_2O_3) BSB glass systems with ranging from 2 mol % are prepared using melt quenching technique. The FTIR spectral studies confirms the presence of various contents of borate glasses samples. The FTIR spectrum of broad absorption bands identifies the wide distribution of borate structural units. The effects is attributed due to the incorporation of WO_3 and Bi_2O_3 contents on the structures glass samples. The UV-visible study identifies increasing band gap energies of glass specimen confirming their amorphous nature and suggesting their nature of rigidity while the SEM evaluation clearly emphasizes the surface morphology of the glass specimens.

REFERENCES

1. S. Sanghi, S. Duhan, A. Agarwal and P. Aghamkar, *J. Alloys Compd.*, **488**, 454 (2009); https://doi.org/10.1016/j.jallcom.2009.09.009.
2. B. Wang, J. Nisar, C.G. Almeida, A.J.S. Mascarenhas, L.A. Silva, D.G.F. David, P. Bargiela, C.M. Araujo, R. Ahuja and A.F. da Silva, *Phys. Status Solidi B*, **251**, 1034 (2014); https://doi.org/10.1002/pssb.201350265.
3. A.A. Abou Shama and F.H. El-Batal, *Egyptian J. Solids*, **29**, 49 (2006).
4. W.A. Pisarski, J. Pisarska, G. Dominiak-Dzik and W. Ryba-Romanowski, *J. Phys. Condens. Matter*, **16**, 6171 (2004); https://doi.org/10.1088/0953-8984/16/34/016.
5. R. Parmar, R.S. Kundu, R. Punia, P. Aghamkar and N. Kishore, *Physica B*, **450**, 39 (2014); https://doi.org/10.1016/j.physb.2014.05.056.
6. V. Sharma, S.P. Singh, G.S. Mudahar and K.S. Thind, *N.J. Glass Ceramics*, **2**, 133 (2012); https://doi.org/10.4236/njgc.2012.24022.
7. F.L. Galeener, G. Lucovsky and J.C. Mikkelsen Jr., *Phys. Rev. B*, **22**, 3983 (1980); https://doi.org/10.1103/PhysRevB.22.3983.
8. M.C. Weinberg, *J. Non-Cryst. Solids*, **127**, 151 (1991); https://doi.org/10.1016/0022-3093(91)90137-U.
9. D. Boudlich, L. Bih, M.E.H. Archidi, M. Haddad, A. Yacoubi, A. Nadiri and B. Elouadi, *J. Am. Ceram. Soc.*, **85**, 623 (2002); https://doi.org/10.1111/j.1151-2916.2002.tb00141.x.
10. E.I. Kamitsos, A.P. Patsis, M.A. Karakassides and G.D. Chryssikos, *J. Non-Cryst. Solids*, **126**, 52 (1990); https://doi.org/10.1016/0022-3093(90)91023-K.
11. R.D. Husung and R.H. Doremus, *J. Mater. Res.*, **5**, 2209 (1990); https://doi.org/10.1557/JMR.1990.2209.
12. W.H. Dumbaugh, *Phys. Chem. Glasses*, **27**, 119 (1986).
13. F.H. El Batal, *Nucl. Instrum. Methods*, **254**, 243 (2007); https://doi.org/10.1016/j.nimb.2006.11.043.
14. I. Ardelean, S. Cora, R. Ciceo Lucacel and O. Hulpus, *Solid State Sci.*, **7**, 1438 (2005); https://doi.org/10.1016/j.solidstatesciences.2005.08.017.
15. E.I. Kamitsos, M.A. Karakassides and A.P. Patsis, *J. Non-Cryst. Solids*, **111**, 252 (1989); https://doi.org/10.1016/0022-3093(89)90288-3.
16. N.O. Dantas, W.E.F. Ayta, A.C.A. Silva, N.F. Cano, S.W. Silva and P.C. Morais, *Spectrochim. Acta A Mol. Biomol. Spectrosc.*, **81**, 140 (2011); https://doi.org/10.1016/j.saa.2011.05.074.
17. Y. Ito, K. Miyauchi and T. Oi, *J. Non-Cryst. Solids*, **57**, 389 (1983); https://doi.org/10.1016/0022-3093(83)90426-X.
18. A. Beganskiene, V. Sirutkaitis, M. Kurtinaitiene, R. Juskenas and A. Kareiva, *Mater. Sci. (Medziagotyra)*, **10**, 287 (2004).
19. A.E. Morales, E.S. Mora and U. Pal, *Rev. Mex. Fisica*, **S53**, 18 (2007).
20. G. David, R. Luo, M.S. Head and M.K. Gilson, *J. Phys. Chem. B*, **103**, 1031 (1999); https://doi.org/10.1021/jp983675l.
21. M.W. Mackenzie, Advances in Applied Fourier Transform Infrared Spectroscopy, John Wiley, New York (1988).
22. N.B. Colthup, L.W. Daly and S.E. Wiberley, Academic Press, San Diego, edn 3 (1990).
23. P. Kubelka, *J. Oct. Soc. Am.*, **38**, 448 (1948); https://doi.org/10.1364/JOSA.38.000448.
24. P. Kubelka and F. Munk, *Z. Tech. Phys.*, **12**, 593 (1931).
25. X. Gao and I. Wachs, *J. Phys. Chem. B*, **104**, 1261 (2000); https://doi.org/10.1021/jp992867t.
26. Von W.N. Delgass, G.L. Haller, R. Kellerman and J.H. Lunsford, Spectroscopy in Heterogeneous Catalysis, Acadamic Press: New York, p. 86 (1979).
27. B. Eraiah, *Bull. Mater. Sci.*, **29**, 375 (2006); https://doi.org/10.1007/BF02704138.
28. N. Mukherjee, B. Show, S.K. Maji, U. Madhu, S.K. Bhar, B.C. Mitra, G.G. Khan and A. Mondal, *J. Mater. Lett.*, **65**, 3248 (2011); https://doi.org/10.1016/j.matlet.2011.07.016.
29. S. Valencia, J.M. Marín and G. Restrepo, *The Open Mater. Sci. J.*, **4**, 9 (2010); https://doi.org/10.2174/1874088X01004010009.
30. S. Kumar, Z. Jindal, N. Kumari and N.K. Verma, *J. Nanopart. Res.*, **13**, 5465 (2011); https://doi.org/10.1007/s11051-011-0534-5.
31. G. Sharma, K. Singh, Manupriya, S. Singh, H. Singh and S. Bindra, *Radiat. Phys. Chem.*, **75**, 959 (2006); https://doi.org/10.1016/j.radphyschem.2006.02.008.
32. S.E. Aw, H.S. Tan and C.K. Ong, *J. Phys. Condens. Matter*, **3**, 8213 (1991); https://doi.org/10.1088/0953-8984/3/42/016.